

Charge Density Distribution in Tetrasulfur Tetraimide ($S_4(NH)_4$)

David Gregson, Gerhard Klebe, and Hartmut Fuess*

Contribution from the Institut für Kristallographie und Mineralogie der Universität Frankfurt am Main, Senckenberganlage 30, D-6000 Frankfurt am Main, West Germany.
Received February 8, 1988

Abstract: The electron deformation density in tetrasulfur tetraimide ($S_4(NH)_4$, orthorhombic, $Pbnm$ (No. 62), $a = 6.694$ (1) Å, $b = 7.850$ (1) Å, $c = 12.168$ (4) Å, $Z = 4$) was determined by X-ray diffraction. The data were collected on a Nonius CAD-4 diffractometer at 0.71069 Å (Mo $K\alpha$, graphite monochromator) and 103 K (11158 measurements, 3009 unique with $F^2 > 0$, $(\sin \theta_{\max})/\lambda = 1.25 \text{ \AA}^{-1}$). Extensive intermolecular hydrogen bonding in the solid state destroys the 4mm chemical symmetry of the isolated molecule. The intermolecular deformation density provides direct evidence for the existence of these hydrogen bonds. Differences in the shape and size of the charge density accumulation within the molecule and the amplitudes of thermal vibration at sites that would be equivalent in the isolated molecule are rationalized in terms of the hydrogen bonding. Bent S-N bonds of order >1.0 and with endocyclic maxima are found.

A brief look at structures containing sulfur-nitrogen bonds reveals a large variation in the S-N bond length, from 1.416 Å in triazol trifluoride¹ to 1.77 Å in sulfamic acid.² This distribution over a range of more than 0.35 Å reflects the ability of the two elements to exist in a variety of bonding states; equally, the bond angles S-N-S and N-S-N vary widely (see S_4N_4 ,³ $(SF)_4N_4$,⁴ and $S_4(NH)_4$, this paper). Karpfen et al.⁵ proposed a classification based on a linear relationship between bond length and bond order; they assigned distances of 1.73 Å corresponding a bond order of 1.0, 1.56 Å to 2.0, and 1.50 Å to 2.5. Apart from the linear relationships, functions with exponential and hyperbolic terms have been successfully employed to correlate bond order with bond length in experimental data.⁶⁻⁸ However, as experimental evidence indicates a continuous change in bonding geometry around S and N throughout the various compounds, these findings should be reflected in pronounced variations of the electron distribution around the two elements. Accordingly, single bonds are to be expected throughout the eight-membered S-N ring. Compared with the above-mentioned value of 1.73 Å for a S-N single bond in sulfamic acid, the distances in $S_4(NH)_4$ are remarkably shortened and a priori a bond order greater than 1 should be assigned. Similar findings hold for bonds between other third-row main-group elements such as Al, Si, and P and electronegative species such as N, O, and F. Experimental investigations⁹⁻¹¹ show a charge density distribution that is not cylindrically symmetric with respect to the internuclear vector; i.e., the bond is somehow bent. Theoretical calculations on $S_4(NH)_4$ ¹² predicted bent bonds between S and N with their maxima outside the direct internuclear vector. An experimental charge density study in the crystalline phase was performed in order to elucidate any evidence of bent bonds between S and N, which then would explain why a bond order greater than 1.0 is assigned for the directly measured internuclear S-N distance in $S_4(NH)_4$.

Experimental Section

The title compound was prepared from S_4N_4 by reduction with $SnCl_2$. Suitable crystals were obtained by recrystallization from benzene. A

Table I. Crystal Data for $S_4(NH)_4$

space group	$Pbnm$ (No. 62)
temp, K	103
a , Å	6.694 (1)
b , Å	7.850 (1)
c , Å	12.168 (4)
V , Å ³	639.3 (3)
measd reflections	11158
unique reflections	3009
μ , cm ⁻¹	13.30
radiation	Mo $K\alpha$ (0.71069 Å)

crystal with dimensions $0.57 \times 0.25 \times 0.24 \text{ mm}^3$ was selected for data collection and mounted in a glass capillary on a Nonius CAD-4 single-crystal diffractometer. Unit-cell constants at 103 K (Table I) were determined by least-squares refinement against the setting angles of 25 centered reflections. A Nonius cold nitrogen gas flow device was used to maintain the temperature at $103 \pm 3 \text{ K}$. A thermocouple mounted in the cold stream was calibrated by using the phase transition of KH_2PO_4 at 122.7 K. The integrated intensities were derived by the method of Lehmann and Larsen;¹³ intensity fluctuations of the three standard reflections (0,2,-7, 1,6,4 -2,0,-8) did not exceed $\pm 3\%$. An absorption correction was carried out by using the ABCOR link¹⁴ of the XRAY suite of programs. Symmetry-equivalent observations from the 11158 measured intensities were averaged, leaving a unique set of 3009 reflections, where $R_{\text{merge}} = 0.016$. The coordinates obtained by Sabine and Cox¹⁵ were used as a starting model for the refinements.

Least-Squares Refinements. All refinements described below were carried out against $|F_o|$, and data with $F^2 > 0$ were used. The scattering factors were those of Fukamachi,¹⁶ and in the case of the deformation refinements the scattering factors for S and N were split into core and valence contributions. A summary of the more important refinements is given in Table II.

Conventional Refinement. A standard refinement using the full-matrix, least-squares program UPALS¹⁷ was carried out with anisotropic thermal parameters for sulfur and nitrogen and independent isotropic thermal parameters for hydrogen. The refined positions of the nitrogen and hydrogen atoms were used to define the N-H vectors, which in turn were used to calculate the positions of the hydrogen nuclei. This refinement also served to establish an extinction parameter.

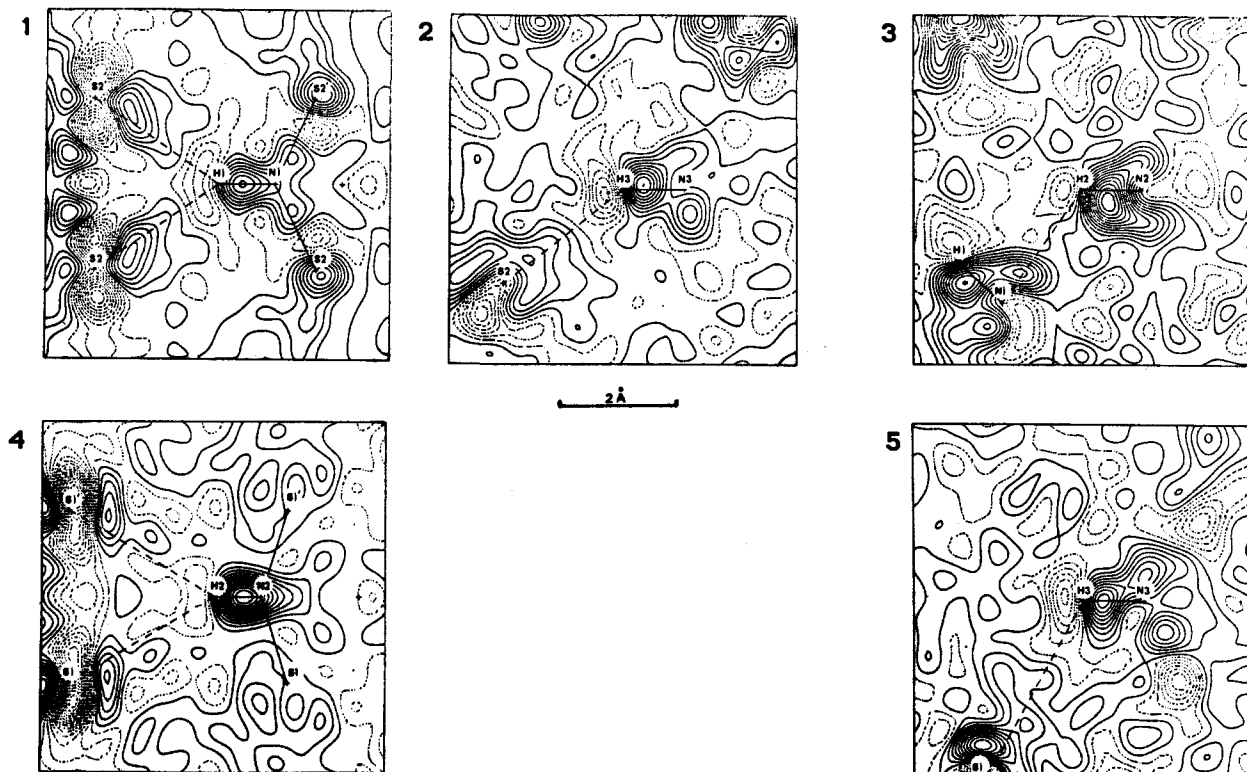
High-Order Refinements. The positional and thermal parameters of sulfur and nitrogen were determined by a series of high-order refinements. Data with $(\sin \theta_{\min})/\lambda = 0.8, 0.9, \text{ and } 1.0 \text{ \AA}^{-1}$ were used in three refinements to define the required parameters. The model included hydrogen atoms at their (fixed) nuclear positions and a fixed, isotropic

- (1) Glemser, O. *Angew. Chem.* **1963**, *75*, 697.
- (2) Bats, J. W.; Coppens, P.; Koetzle, T. F. *Acta Crystallogr., Sect. B* **1977**, *B33*, 37.
- (3) Sharma, B.; Donohue, J. *Acta Crystallogr.* **1963**, *16*, 891.
- (4) Wieggers, G. A.; Vos, A. *Acta Crystallogr.* **1963**, *16*, 152.
- (5) Karpfen, A.; Schuster, P.; Petkov, J.; Lisdika, H. *J. Chem. Phys.* **1978**, *68*, 3884.
- (6) Pauling, L. *The Nature of the Chemical Bond*; Cornell University Press: Ithaca, NY, 1960.
- (7) Donnay, G.; Allmann, R. *Am. Mineral.* **1970**, *55*, 1003.
- (8) Shannon, R. D. *Acta Crystallogr., Sect. A* **1973**, *A29*, 266.
- (9) Bats, J. W.; Fuess, H. *Acta Crystallogr., Sect. B* **1986**, *B42*, 26.
- (10) Bats, J. W.; Fuess, H.; Elerman, Y. *Acta Crystallogr., Sect. B* **1986**, *B42*, 552.
- (11) Klebe, G.; Bats, J. W.; Fuess, H. *J. Am. Chem. Soc.* **1984**, *106*, 5202.
- (12) Foti, A. E.; Smith, V. H.; Kishner, S.; Gopinathan, M. S.; Whitehead, M. A. *Mol. Phys.* **1978**, *1*, 111.

- (13) Lehmann, M. S.; Larsen, F. K. *Acta Crystallogr., Sect. A* **1974**, *A30*, 580.
- (14) Alcock, N. W. In *Crystallographic Computing*; Ahmed, F. R., Ed.; Munksgaard: Copenhagen, 1970.
- (15) Sabine, T. M.; Cox, G. W. *Acta Crystallogr.* **1967**, *23*, 574.
- (16) Fukamachi, T. Technical Report B12, Institute for Solid State Physics, University of Tokyo, 1970.
- (17) Lundgren, J.-O. *UPALS, Crystallographic Computer Programs*, Report UUIC-B13-4-04, Institute of Chemistry, University of Uppsala, 1982.

Table II. Summary of Least-Squares Refinements

refinement	$N(\text{obsd})$	$N(\text{var})$	$R(F)$	$R_w(F)$	GOF	comments
conventional, all data	3009	42	0.033	0.032	1.86	S and N anisotropically refined; H isotropically refined; isotropic extinction; weight = $1/\sigma^2(F)$, where $\sigma(F^2) = [\sigma(F^2)^2 + (0.01F^2)^2]^{1/2}$
high-order, $(\sin \theta_{\text{min}})/\lambda = 0.9 \text{ \AA}^{-1}$	995	40	0.058	0.027	1.42	determination of structural parameters of S and N without bias from valence electron scattering; weight as above
high-order, $(\sin \theta_{\text{min}})/\lambda = 0.9 \text{ \AA}^{-1}$; third-order cumulants	995	82	0.057	0.026	1.30	attempt to model "librational" motion; no significant coefficients for third-order cumulants; weight as above
deformation refinement using all data; Coppens and Hansen formalism	3009	152	0.029	0.016	1.45	all crystallographically allowed populations on S and N up to hexadecapoles; H with monopoles and bond-directed dipoles; STO (four types) refined; weight as above
deformation refinement using all data; Hirshfeld formalism	3009	193	0.028	0.026	1.46	as above, but six atom types with fixed STO coefficients

Figure 1. Intermolecular X-X' deformation density. Contour interval $0.05 e \text{ \AA}^{-3}$; negative contours dashed.

extinction parameter. The goodness of fit became better with increasing cut-off angle but since there were only 286 reflections above 1.0 \AA^{-1} , and this gave a low observation to parameter ratio, the parameters from the refinement with $(\sin \theta_{\text{min}})/\lambda = 0.9 \text{ \AA}^{-1}$ were used for subsequent calculation of structure factors and generation of X-X' maps.

An attempt to describe a suspected librational motion using atom-centered third-order cumulants was made. Again, data with $(\sin \theta_{\text{min}})/\lambda > 0.9 \text{ \AA}^{-1}$ were used, giving an acceptable observation to parameter ratio of about 12. However, the coefficients of the third-order cumulants were not significant—the largest of them barely attained 2 standard deviations. More importantly, there was no sign that the atoms with the larger thermal motion showed any tendency to have the larger coefficients, and the anisotropic harmonic thermal parameters were virtually unchanged by the inclusion of the anharmonic terms.

Deformation Refinements. Local coordinate systems (LCS) were defined for each atom to reflect as nearly as possible the molecular geometry at the site. All crystallographically allowed population parameters were refined in the cases of sulfur and nitrogen but the hydrogen atoms were constrained to have cylindrical symmetry about the N-H bond. No chemical equivalence was assumed; i.e., each atom was allowed to refine with its own set of population parameters.

Two programs using different formalisms were employed—MOLLY with the Coppens-Hansen formalism¹⁸ and UPALS using the Hirshfeld formalism.¹⁹ The Hirshfeld deformation functions form a more flexible expansion than those of Coppens and Hansen; thus it might be expected

that the UPALS refinement should give a result at least as good as that obtained from MOLLY. Although convergence was reached in both cases, the results were not identical, and the MOLLY refinement seemed better. One possible explanation for this is that the Slater type orbital (STO) exponents refined sensibly in MOLLY but any attempt at a simultaneous refinement of the exponential coefficients and population parameters with UPALS caused the refinement to diverge. Despite attempts at fixing the population parameters while refining the STO exponents and at using fixed but different STO exponents in a series of refinements of the population parameters, the UPALS result could never match the result obtained from MOLLY. The more convincing result from MOLLY was used in the subsequent generation of model density maps. The final atomic coordinates are given in Table III.

Results

Fourier Maps. The deformation density maps use data up to $(\sin \theta_{\text{max}})/\lambda = 0.7 \text{ \AA}^{-1}$, a total of 964 unique reflections. The program used to calculate the maps was JIMPLAN;²⁰ negative contours are dashed, and zero and positive contours are solid lines. Three types of map were plotted: (1) X-X', where structure factors calculated from the parameters resulting from a high-order refinement were subtracted from the observed structure factors (the observed structure amplitudes were given the phase of the calculated ones), (2) static deformation density maps (the difference density $F_c(\text{multipole}) - F_c(\text{neutral, spherical})$ was plotted,

(18) Hansen, N. K.; Coppens, P. *Acta Crystallogr., Sect. A* **1978**, *A34*, 909.

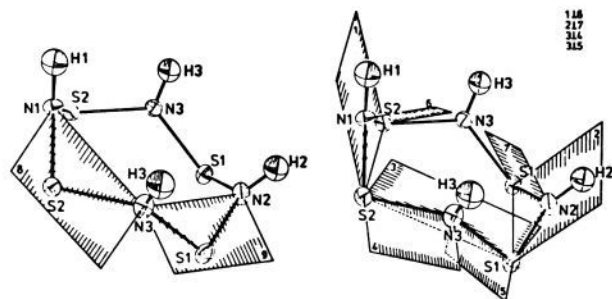
(19) Hirshfeld, F. *Isr. J. Chem.* **1977**, *16*, 226.

(20) Coppens, P. JIMPLAN, a SUNY Buffalo Crystallographic Computing Program.

Table III. Fractional Coordinates for the Asymmetric Unit in $S_4(NH)_4^a$

atom	x	y	z
S(1)	0.17981 (5)	0.03622 (5)	0.12899 (4)
S(2)	0.75366 (5)	0.13609 (4)	0.12899 (3)
N(1)	0.7145 (3)	0.2325 (2)	0.25
N(2)	0.2697 (2)	0.1025 (3)	0.25
N(3)	0.9914 (2)	0.1634 (2)	0.0914 (2)
H(1)	0.702 (2)	0.344 (2)	0.25
H(2)	0.350 (2)	0.191 (2)	0.25
H(3)	0.017 (2)	0.249 (2)	0.058 (1)
H(1)	0.6896	0.3645	0.25
H(2)	0.3544	0.2143	0.25
H(3)	0.0315	0.2710	0.0456

^aThe refined hydrogen atom parameters are given first followed by the calculated nuclear positions. The latter were used in calculating the hydrogen bond lengths and the maps.

**Figure 2.** Planes for which the static deformation density was calculated.

and the temperature parameters were set to zero to permit comparison of similar chemical sites without interference from thermal smearing), and (3) residual density maps ($F_o - F_c$ (multipole) maps were plotted). The intermolecular charge density in the hydrogen bonds is illustrated in Figure 1 by the X-X' technique. The intramolecular charge density is shown in Figure 3; this is the static model deformation density for the planes given in Figure 2. The corresponding residual density is shown in Figure 4.

The errors in maps produced by Fourier techniques have been discussed at length in the literature; see, e.g., ref. 21–23. Assuming that the correlations between $\rho(\text{obsd})$, $\rho(\text{calcd})$, and the scale factor k are negligible, the variance in the deformation density is given by the expression

$$\sigma^2(\Delta\rho) = [1/k^2]\sigma^2(\rho_o) + \left[\frac{\sigma^2(k)}{k^2} \right] \rho_o^2 + \sigma^2(\rho_c)$$

The first term on the right-hand side of the equation is nearly constant over the unit cell and makes the main contribution to the errors at distances $>0.5 \text{ \AA}$ from the atomic nuclei. The second term becomes large when $\rho(\text{obsd})$ becomes large and thus renders features near the atomic nuclei virtually meaningless. The third term contains the errors introduced by the model, which are close to zero away from the atoms and fairly large near them. The value of the first term on the right-hand side may be calculated from the approximation given by Cruickshank²⁴

$$\sigma^2(\rho_o) = \frac{2}{V^{1/2}} \sum \sigma^2(5F_o)$$

where the summation is over half of reciprocal space out to the resolution of the maps. This gives an approximate esd of 0.05 e \AA^{-3} (calculated value = 0.044 e \AA^{-3}) in the bonding regions. In addition, a series of maps was plotted, using the X-X' technique, in which there was a small change of scale factor in otherwise identical maps. The results showed that although the features at the atomic sites change markedly, the interatomic features were

Table IV. Some Intramolecular Contact Distances (\AA), Intermolecular Contact Distances (\AA) and Angles (Deg), and Best Planes in the Crystal Structure of $S_4(NH)_4^a$

(a) Intramolecular Nonbonded Contacts			
atoms	distance	atoms	distance
S(1)···S(2)	2.9598 (5)	S(1)···H(2)	2.322 (5)
S(1)···S'(1)	2.9473 (7)	S(1)···H(3)	2.305 (7)
N(1)···N(3)	2.730 (2)	S(2)···H(1)	2.335 (5)
N(2)···N(3)	2.727 (2)	S(2)···H(3)	2.345 (7)
(b) Intermolecular Contact Distances and Angles			
atoms	distance	angle	
N(1)–H(1)···S(2)	2.619 (6)	126.3 (4)	
N(3)–H(3)···S(2)	2.694 (9)	141.2 (6)	
N(2)–H(2)···S(1)	2.933 (6)	132.9 (3)	
H(3)–H(3)···S(1)	3.016 (7)	122.9 (6)	
N(2)–H(2)···N(1)	2.414 (6)	126.3 (4)	
(c) Some Least-Squares Planes of Interest			
atom	dev from plane, \AA	eq of plane in orthogonal angstrom space	
S(1)	–0.0263	0.7612x – 0.6485y = 5.8553	
S'(1)	–0.0263		
N(2)	0.0935		
H(2)	–0.0409		
S(2)	0.0162	0.9712x + 0.2385y = 5.1372	
S'(2)	0.0162		
N(1)	–0.0580		
H(1)	0.0255		
S(1)	0.0060	0.1483x + 0.5381y + 0.8298z = 2.6181	
S(2)	0.0063		
N(3)	–0.0218		
H(3)	0.0094		

^aAs a reference the corresponding van der Waals radii amount to $r(S) = 1.85 \text{ \AA}$, $r(N) = 1.50 \text{ \AA}$, and $r(H) = 1.20 \text{ \AA}$ (taken from ref 37).

left largely unaltered. The interpretation of features larger than 0.15 e \AA^{-3} in the bonding regions thus seems reasonable.

Molecular Structure. The molecular and crystal structure of $S_4(NH)_4$ was first determined by Sass and Donohue in 1957. A neutron diffraction study by Sabine and Cox in 1967 revealed the hydrogen positions. The results of our X-ray study are in agreement with the observations of these two studies; the molecular geometry, bond lengths, and bond angles are shown in Figure 5. The intramolecular contact distances that are less than the sum of the corresponding van der Waals radii are given in Table IVa. The calculation of the intra- and intermolecular contact distances was carried out with the hydrogen atoms at their nuclear positions. The nuclear coordinates themselves were calculated from the observed X-ray ones by projecting along the N–H vectors in the ratio of 1.02 \AA to the observed bond length; 1.02 \AA is a typical value for a N–H bond length determined by neutron diffraction.^{26–29} Sabine and Cox¹⁵ found the following distances: N1–H1 = $1.08 (5) \text{ \AA}$; N2–H2 = $0.96 (5) \text{ \AA}$; N3–H3 = $1.08 (3) \text{ \AA}$. A similar pattern is not observed in our X-ray-determined bond lengths, which have smaller standard deviations, and so the neutron values were not taken to be reliable. The low-temperature cell dimensions are smaller than those determined by Sass and Donohue for the room-temperature structure, which were used by Sabine and Cox. Our internuclear S–N distances, however, are longer than those of Sabine and Cox for S(1)–N(2), S(1)–N(3), and S(2)–N(1), although shorter for S(2)–N(3). This may be explained by the fairly imprecise bond lengths derived from the

(21) Rees, B. *Acta Crystallogr., Sect. A* **1976**, *A32*, 483.(22) Stevens, E. D.; Coppens, P. *Acta Crystallogr., Sect. A* **1976**, *A32*, 915.(23) Rees, B. *Isr. J. Chem.* **1977**, *16*, 180.(24) Cruickshank, D. W. J. *Acta Crystallogr.* **1949**, *2*, 65.(25) Sass, R. L.; Donohue, J. *Acta Crystallogr.* **1958**, *11*, 497.(26) Hamilton, W. C.; La Placa, S. J. *Acta Crystallogr., Sect. B* **1968**, *B24*, 1147.(27) Hamilton, W. C. *Annu. Rev. Phys. Chem.* **1962**, *13*, 19.(28) Cohen-Addad, C.; Savariault, J.-M.; Lehmann, M. S. *Acta Crystallogr., Sect. B* **1981**, *B37*, 1703.(29) Kvick, A.; Thomas, R.; Koetzle, T. F. *Acta Crystallogr., Sect. B* **1976**, *B32*, 224.

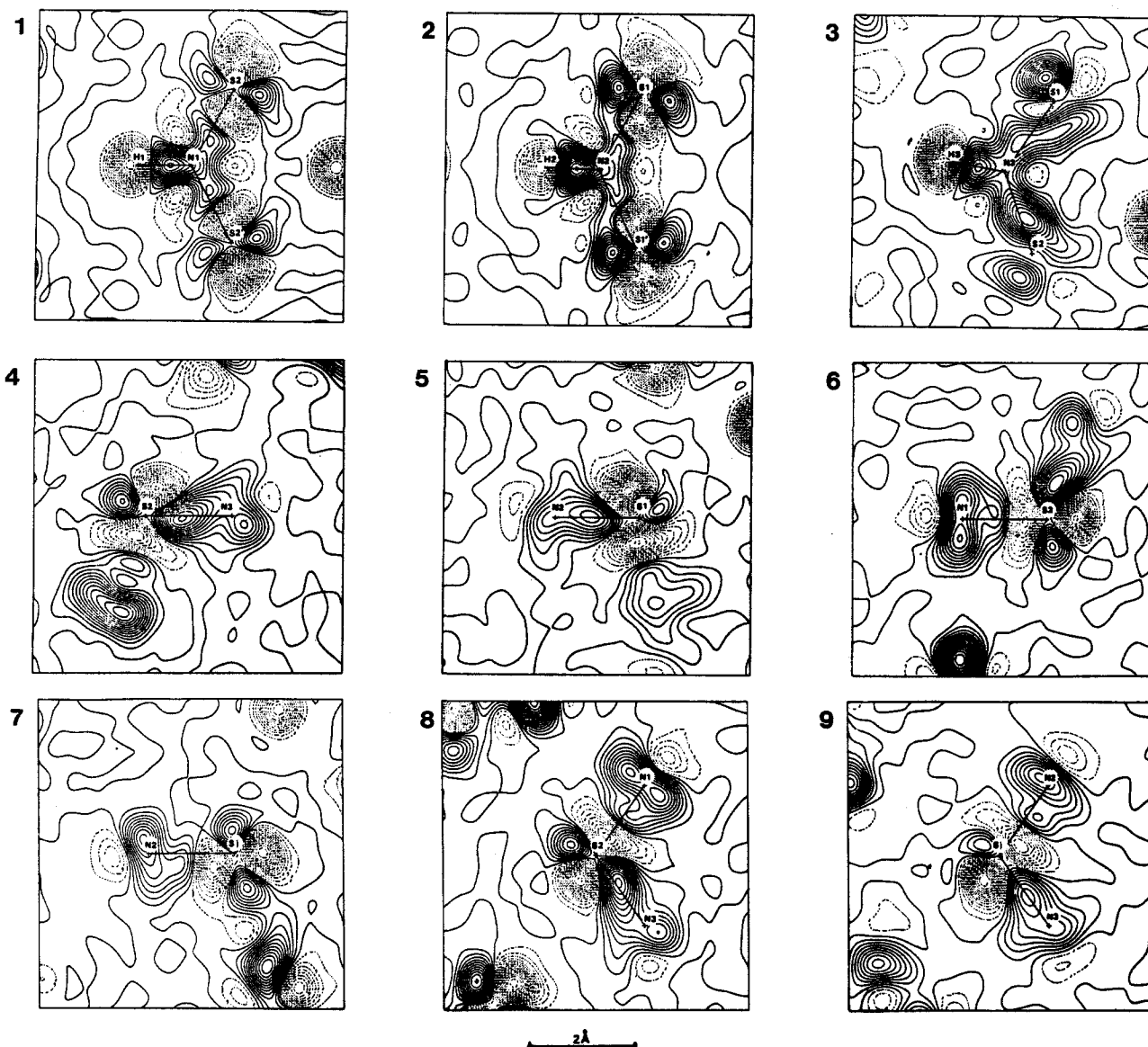


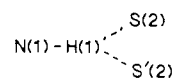
Figure 3. Static model deformation density. Contours as in Figure 1.

neutron study, where the S-N average is 1.66 Å with a sample standard deviation (ssd) of 0.03. The bond lengths given by Sass and Donohue are more internally consistent with an average of 1.675 Å and ssd of 0.006. This compares well with our study, where the average S-N distance is 1.673 Å with an ssd of 0.002. In view of the very small difference between the room-temperature and low-temperature S-N distance, the cell contraction is probably due to the reduction of intermolecular distances.

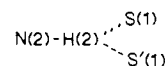
Hydrogen Bonds. According to Hamilton and Ibers,³⁰ a good working definition for the existence of a hydrogen bond is that at least two heavy atom-hydrogen atom distances less than the sum of the van der Waals radii be present. There is also a rather loose requirement that the bond be linear. Kroon et al.³¹ and Pedersen³² showed that the number of hydrogen bonds per solid angle as a function of X-H...Y angle gives an approximately Gaussian distribution centered about the interval $175^\circ < X-H...Y < 180^\circ$. It should not be implied, however, that the most stable configuration always involves a linear bond, particularly if the bond is weak. The balance between efficient molecular packing and distortion of hydrogen bonds will determine the most favorable arrangement. With the above criteria, there are five different

hydrogen bonds found in the solid state of $S_4(NH)_4$; they are listed in Table IVb. We find evidence in the deformation density for three of them, which are illustrated in Figure 6.

The bifurcated bond



is the shortest of the S...H type (2.62 Å), and polarization of the density at S(2) toward H(1) can be seen (Figure 1.1); the accumulation of density in the S...H region is large. In N(3)-H(3)...S(2) (2.70 Å), polarization of density at S(2) can be seen (Figure 1.2), although it is more diffuse than the first case. The two long hydrogen bonds (Figure 1.4,5) show no convincing buildup of density. The bifurcated bond (2.93 Å)



has a small peak pointing toward S(1) but the height is not significant. The density in N(3)-H(3)...S(1) (3.02 Å) is very diffuse and nondirectional; the H...S distance is only marginally less than the sum of the van der Waals radii (see Table IV). The short N...H bond, N(2)-H(2)...N(1) (2.41 Å (Figure 1.3)), has a large, well-defined accumulation of density near N(1). The polarizability of N is less than that of S, which accounts for the less diffuse nature of the bonding density in N...H. It is also

(30) Hamilton, W. C.; Ibers, J. A. *Hydrogen Bonding in Solids*; W. A. Benjamin: San Francisco, 1968.

(31) Kroon, J.; Kanters, J. A.; van Duijneveldt-van de Rijdt, J. G. C. M.; van Duijneveldt, F. B.; Vliegenhart, J. A. *J. Mol. Struct.* **1975**, *24*, 109.

(32) Pedersen, B. *Acta Crystallogr., Sect. B* **1974**, *B30*, 289.

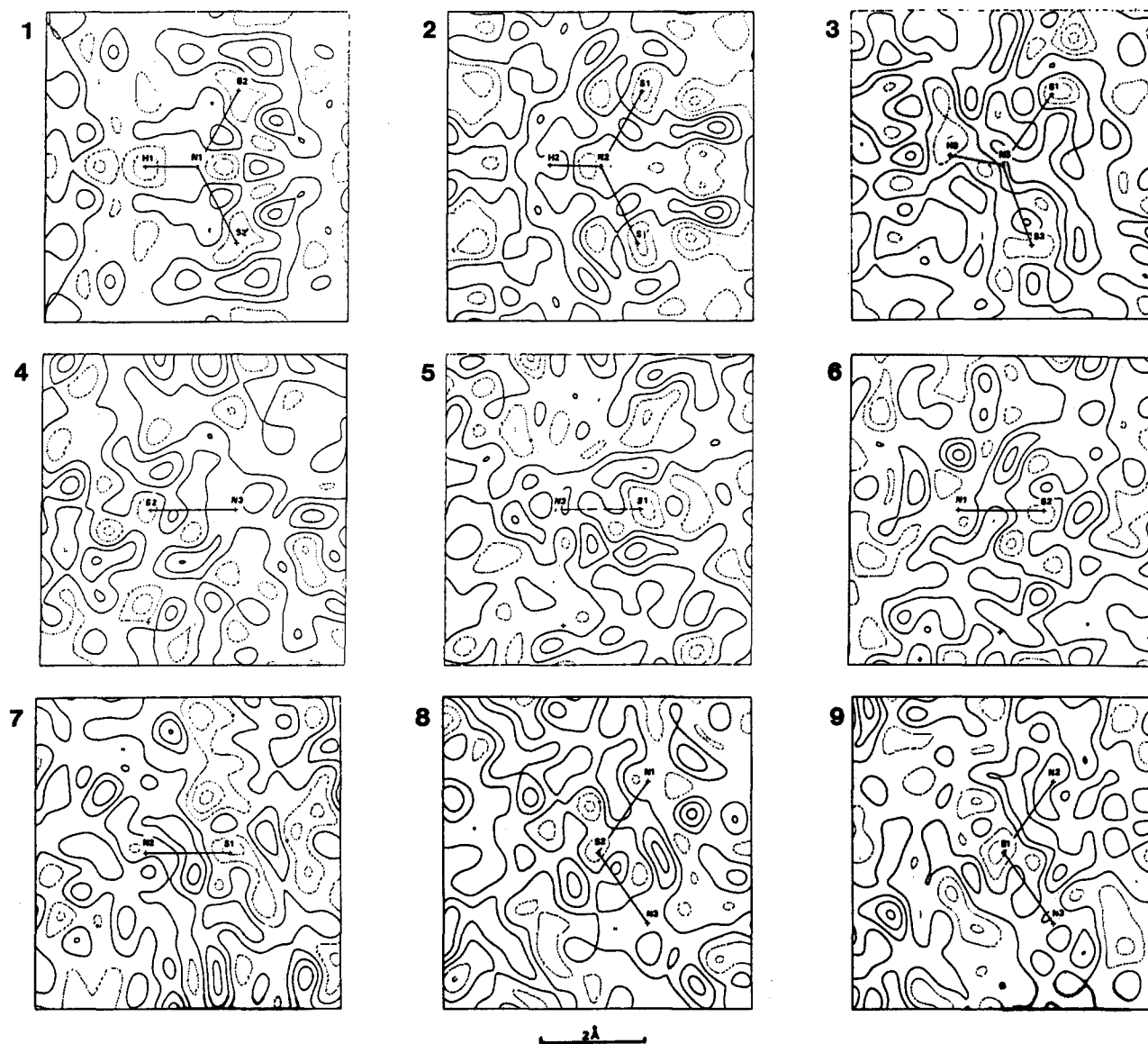


Figure 4. Residual density corresponding to the sections in Figures 2 and 3. Contours as in Figure 1.

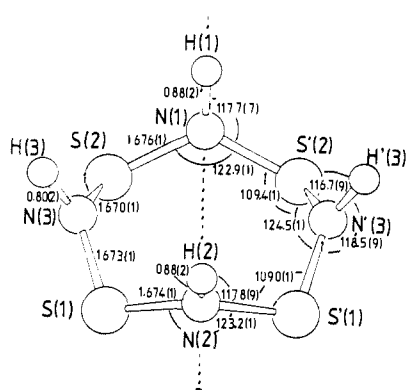


Figure 5. Molecular geometry with bond lengths and angles shown.

interesting to note that the bonding density in N(2)-H(2) is off axis, possibly as a result of the polarizing influence of N(1).

Discussion

Our results show that the bond maxima in the deformation density are endocyclic (Figure 3.1-3). The densities in Figure 3.1 and 3.2 represent almost the same plane with regard to the hybridization at the S atom whereas the plane of Figure 3.3 is almost perpendicular (see Figure 2). The S-N distances that pass through the bond maxima are 1.68-1.70 Å, which is less than the

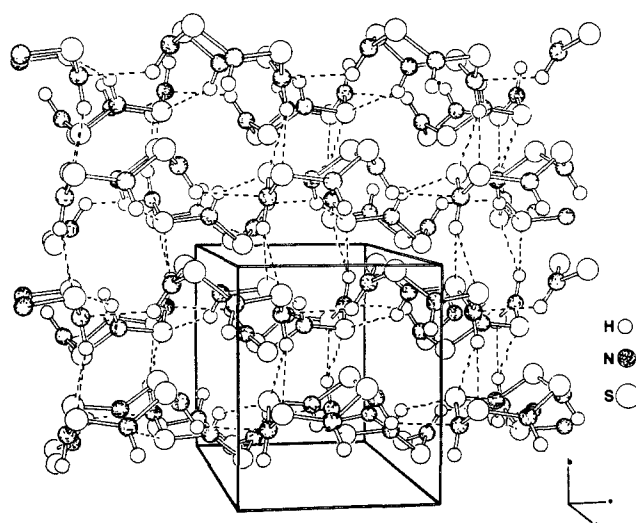
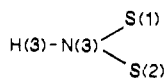


Figure 6. View of the packing and hydrogen bonding. Only the three H bonds for which clear evidence was seen in the deformation density have been included.

S-N bond in sulfamic acid (1.77 Å, (ref 2)) and also less than the value of 1.73 Å proposed for a single bond by Karpfen et al.;⁵ thus the bond order is greater than 1.0. Foti et al.¹² proposed a

hybridization scheme for the bonding that would require bent S–N bonds of order ~ 1.0 with exocyclic maxima; we agree that the bonds are bent but not with the bond order or position of the maxima. The bonds are, however, longer than the direct internuclear S–N distance, showing that the simple linear relationship between bond length (internuclear distance) and bond order is an oversimplification that should be treated with caution. Thus we are led to the conclusion that there is some degree of double bonding present; the question remains as to what causes it. The diffuseness of sulfur d orbitals has been used as an argument against their involvement,³³ since the overlap at distances relevant to bonding would be small. However, recent work by Cruickshank and Eisenstein on sulfamic acid and SO_3 ,³⁴ and SO_2 , NO_2 , and their ions,³⁵ has shown that d functions in ab initio calculations are necessary for a proper description of the molecular geometry and deformation density³⁶ in molecules containing first- or second-row atoms, although their contribution is much larger in the latter. Cruickshank and Eisenstein draw an analogy between atomic d orbitals and the calculated molecular orbitals that have pure or high contribution from d functions, which represent the atomic d orbitals in the basis set, to explain how the bonding is affected by d orbitals. Atomic d orbitals have intrinsic angular orthogonality to all atomic s and p orbitals and can thus penetrate the core region of the atom. For both S and N ($s^2p^3d^1$ and $s^2p^2d^1$, respectively), the effective nuclear charge experienced by the 3d orbital outside the core is about 1 e; but inside the core, the sulfur orbital experiences a greater effective nuclear charge than the nitrogen orbital (because of the greater nuclear charge on S), and this over a greater radius (because S(1s2s2p) is larger than N(1s)). Therefore the more attractive inner region potential of sulfur enhances the amplitude of the 3d orbital at distances relevant to bonding. In our study, the involvement of the sulfur d orbital is implied by the length of the S–N bond.

The Hydrogen Bonds. It is not surprising that the extensive intermolecular hydrogen bonding has an effect upon the deformation density within the molecule. At S(2), there are two lobes of density, one of which is due to polarization by H(1) (Figure 1.1), the other by H(3) (Figure 1.2); these correspond to the two short S...H bonds. The S(1) atom has the two long S...H interactions, and the existence of one weak lobe of density, toward H(2) (Figure 1.4), and the nondirectional diffuse cloud between S(1) and H(3) (Figure 1.5) suggest that these interactions do not constitute hydrogen bonds. One result of this asymmetry in the hydrogen bonding is the destruction of the chemical mirror that would pass through H(3)–N(3)–N(3)'–H(3)' in the asymmetrical isolated molecule, giving the distorted deformation density (Figure 3.3) in the plane



The different environments produced by hydrogen bonding at apparently chemically equivalent sites within the molecule may

lead to such features as different amplitudes of thermal vibration for atoms that would be the same in the isolated molecule. It was mentioned above that this difference could have been due to a rigid-body motion but that attempts to model it as such were not successful.

Interpretation in terms of the hydrogen bonds appears to be reasonable. S(2) is involved in two strong hydrogen bonds, whereas S(1) is not and the trace of the U_{ij} matrix for S(2) is significantly smaller than that of S(1); thus the apparent explanation is that S(2) is simply more firmly anchored by the stronger bonds than is S(1). The same argument can be applied to the N atoms in the molecule—the traces of the U_{ij} matrices are in the order $N(1) < N(3) < N(2)$. Here, N(1) is involved in a hydrogen bond but the other two are not.

Conclusion

We find evidence for bent S–N bonds with endocyclic maxima. The bond lengths, passing through the S–N maxima, are between 1.68 and 1.70 Å, which shows that the bond order is greater than 1. The partial double-bond character is probably due to the involvement of the sulfur d orbitals, as discussed by Cruickshank and Eisenstein.³⁵

An important conclusion to be drawn from this study is that the molecule in the solid state cannot naively be compared to the isolated molecule. There is ample evidence in this study of intermolecular hydrogen bonds causing polarization of electron density and consequent rearrangement of the intramolecular bonding density. Thus chemical symmetry that may exist in the isolated molecule does not exist in the solid state. A corollary of this is that taking the average deformation density over supposedly equivalent sites should be carried out only if it is certain that equivalence exists. Equally, the method of reducing the number of variable parameters in least-squares refinements by similar assumptions about chemical equivalence should be employed with caution.

Five different hydrogen-bonding schemes exist according to the criteria outlined above. We find clear evidence in the deformation density for the formation of hydrogen bonds in the three shorter ones. The two longer bonds, both of the S...H type, are only 0.12 and 0.02 Å less than the sum of the van der Waals radii and show no convincing evidence for the presence of hydrogen bonding. This agrees with Hamilton and La Placa,²⁶ who suggested that if the H...Y distance is shorter than the sum of the van der Waals radii by about 0.2 Å, then H...Y may be considered to form part of a hydrogen bond. Our results show that when the H...S contact is less than about 0.2 Å shorter than the sum of the van der Waals radii, the unambiguous assignment of a hydrogen bond is not justified and we suggest that for any H...Y contact this may be the case. Further, the linearity condition appears to be a very loose constraint, and the X–H...Y angle, even in the case of relatively strong bonds (e.g., N(2)–H(2)...N(1) in this study), can be far from linear.

Acknowledgment. This work has been supported by the Bundesministerium für Forschung und Technologie and by the Deutsche Forschungsgemeinschaft (Bonn).

Supplementary Material Available: Refined population parameters, definition of local coordinate system, and κ values (2 pages); listing of observed and calculated structure factors based on the multipole refinement (26 pages). Ordering information is given on any current masthead page.

(33) Cruickshank, D. W. J.; Webster, B. C.; Spinnler, M. A. *Int. J. Quantum Chem.* **1967**, *18*, 225.

(34) Cruickshank, D. W. J.; Eisenstein, M. *J. Mol. Struct.* **1985**, *130*, 143.

(35) Cruickshank, D. W. J.; Eisenstein, M. *J. Comput. Chem.* **1987**, *8*, 6.

(36) Fuess, H.; Bats, J. W.; Cruickshank, D. W. J.; Eisenstein, M. *Angew. Chem., Int. Ed. Engl.* **1985**, *24*, 509.

(37) *CRC Handbook of Chemistry and Physics*, 65th ed.; Chemical Rubber Co.: Boca Raton, FL, 1984–1985; p D-191.